multiscale algorithms for the solution of Poisson's equation

Stefan Goedecker

Département de recherche fondamentale sur la matière condensée,
SP2M/L_Sim, CEA-Grenoble, 38054 Grenoble cedex 9, France

1 Abstract

It is shown how various ideas that are well established for the solution of Poisson's equation using plane waves, Fast Multipole and Multigrid methods can be incorporated into the wavelet context. The combination of wavelet concepts and multigrid techniques turns out to be particularly fruitful. We propose a new multigrid V cycle scheme that is not only much simpler, but also more efficient than the standard V cycle. Whereas in the traditional V cycle the residue is passed to the coarser grid levels, this new scheme does not require the calculation of a residue. Instead it works with copies of the charge density on the different grid levels that were obtained from the underlying charge density on the finest grid by wavelet transformations. This scheme is not limited to the pure wavelet setting, where it is faster than the preconditiooned conjugate gradient method, but equally well applicable for finite difference discretizations of Poisson's equation.

2 Introduction

Poisson's equation

$$\nabla^2 V(\mathbf{r}) = -4\pi\rho(\mathbf{r}) \tag{1}$$

is the basic equation for electrostatic problems. As such it plays an important role in a large variety of scientific and technological problems. The solution of the differential equation Eq. 1 can be written as an integral equation

$$V(\mathbf{r}) = \int \frac{\rho(\mathbf{r}')}{|\mathbf{r}-\mathbf{r}'|} \tag{2}$$

Gravitational problems are based on exactly the same equations as the electrostatic problem, but we will use in this article the language of electrostatics, i.e. we will refer to $\rho(\mathbf{r})$ as a charge density. The most efficient numerical approaches for the solution of electrostatic problems are based on Eq /refpoisson rather than Eq. /refinteq. However preconditioning steps found in these methods can be considered as approximate solutions of Eq. /refinteq. The fact that the Green's function $\frac{1}{|\mathbf{r}-\mathbf{r}'|}$ is of long range makes the numerical solution of Poisson's equation difficult, since it implies that a charge density at a point $\mathbf{r}'$ will have an non-negligible influence on the potential $V(\mathbf{r})$ at a point $\mathbf{r}$ far away. A naive implementation of Eq. 2 would therefore have a quadratic scaling. It comes however to our help, that the potential arising from a charge distribution far away is slowly varying and does not depend on the details of the charge distribution. All efficient algorithms for

solving electrostatic problems are therefore based on a hierarchical multiscale treatment. On the short length scales the rapid variations of the potential due to the exact charge distribution of close by sources of charge are treated, on the large length scales the slow variation due to some smoothed charge distribution of far sources is accounted for. Since the number of degrees of freedom decreases rapidly with increasing length scales, one can obtain algorithms with linear or nearly linear scaling. In the following, we will briefly summarize how this hierarchical treatment is implemented in the standard algorithms

- Fourier Analysis:
  If the charge density is written in its Fourier representation

  $$\rho(\mathbf{r}) = \sum_{\mathbf{K}} \rho_{\mathbf{K}} e^{i\mathbf{K}\mathbf{r}}$$

  the different length scales that are in this case given by $\lambda = \frac{2\pi}{K}$ decouple entirely and the Fourier representation of the potential is given by

  $$V(\mathbf{r}) = \sum_{\mathbf{K}} \frac{\rho_{\mathbf{K}}}{K^2} e^{i\mathbf{K}\mathbf{r}} \tag{3}$$

  The Fourier analysis of the real space charge density necessary to obtain its Fourier components $\rho_{\mathbf{K}}$ and the synthesis of the potential in real space from its Fourier components given by Eq. 3 can be done with Fast Fourier methods at a cost of $N\, log_2(N)$ where N is the number of grid points.

- Fast Multipole methods (FMM):
  The Fast Multipole method [1] allows us to calculate the potentials and the forces of a discrete system of charged point particles with linear or nearly linear scaling. It can thus be considered as the solution of Poisson's equation for a charge density that is a sum of delta functions centered at the positions of the particles. The potential and forces have to be evaluated only at the position of the particles. In this method both the charge density and the potential are coarse grained and only these coarse grained quantities are interacting over long distances. The coarse grained quantities are large in spatial extent and have less details, i.e they are smoothed versions of the original charge density. The coarse graining is done recursively, leading to a hierarchy of coarse grained quantities. The spatial extent of these coarse grained quantities at the various levels of the hierarchy and the minimum interaction distance, for which this approximate interaction is considered to be exact, are proportional. The coarse graining is done by a multipole expansion. The Fast Multipole method can also easily be generalized to continuous charge distributions that are sums of Gaussian charge distributions [4].

- Multigrid methods (MG):
  Trying to solve Poisson's equation by any relaxation or iterative method (such as conjugate gradient) on the fine grid on which one finally wants to have the solution leads to a number of iterations that increases strongly with the size of the grid. The reason for this is that on a grid with a given spacing h one can efficiently treat Fourier components with a wavelength $\lambda = \frac{2\pi}{K}$ that is comparable to the the grid spacing h,

but the longer wavelength Fourier components converge very slowly. This increase in the number of iterations prevents a straightforward linear scaling solution of Eq. 1. In the multigrid method, pioneered by A. Brandt [5], one is therefore introducing a hierarchy of grids with a grid spacing that is increasing by a factor of two on each hierarchic level. In contrast to the Fourier and FMM methods where the charge and the potential are directly decomposed into components characterized by a certain length scale, it is the residue that is passed from the fine grids to the coarse grids in the MG method. The residue corresponds to the charge that would give rise to a potential that is the difference between the exact potential and the approximate potential at the current stage of the iteration.

In the following we will now show that all the three above mentioned approaches fit quite naturally into the framework of wavelet multiresolution analysis.

Within wavelet theory [18] one has two possible representations of a function $f(x)$, a scaling function representation

$$f(x) = \sum_j s_j^{Kmax} \phi_j^{Kmax}(x) \tag{4}$$

and a wavelet representation.

$$f(x) = \sum_j s_j^{Kmin}\ \phi_j^{Kmin}(x) + \sum_{k=Kmin}^{Kmax} \sum_j d_j^k\ \psi_j^k(x)\,. \tag{5}$$

In contrast to the scaling function representation, the wavelet representation is a hierarchic representation. The wavelet at the hierarchic level k is related to the mother wavelet ψ by

$$\psi_i^k(x) = \sqrt{2}^k \psi(2^k x - i) \tag{6}$$

The characteristic length scale of a wavelet at resolution level k is therefore proportional to 2^{-k}. A wavelet on a certain level k is a linear combination of scaling functions at the higher resolution level $k+1$

$$\psi_i^k(x) = \sum_{j=-m}^{m} g_j\ \phi_{2i+j}^{k+1}(x) \tag{7}$$

Scaling functions at adjacent resolution levels are related by a similar refinement relation

$$\phi_i^k(x) = \sum_{j=-m}^{m} h_j\ \phi_{2i+j}^{k+1}(x) \tag{8}$$

and hence also any wavelet at a resolution level k is a linear combination of the highest resolution scaling functions. The so-called fast wavelet transform allows us to transform back and forth between a scaling function and a wavelet representation.

Let us now introduce wavelet representations of the potential and the charge density

$$V(x) = \sum_j V_j^{Kmin}\ \phi_j^{Kmin}(x) + \sum_{k=Kmin}^{Kmax} \sum_j V_j^k\ \psi_j^k(x) \tag{9}$$

$$\rho(x) = \sum_j \rho_j^{Kmin}\ \phi_j^{Kmin}(x) + \sum_{k=Kmin}^{Kmax} \sum_j \rho_j^k\ \psi_j^k(x) \tag{10}$$

Different levels do not completely decouple, i.e the components on level k, V_j^k, of the exact overall solution do not satisfy the single level Poisson equation

$$\nabla^2 \left(\sum_j V_j^k \ \psi_j^k(x) \right) \neq -4\pi \left(\sum_j \rho_j^k \ \psi_j^k(x) \right) \tag{11}$$

within the chosen discretization scheme. This is due to the fact that the wavelets are not perfectly localized in Fourier space, i.e. many frequencies are necessary to synthesize a wavelet. However the amplitude of all these frequencies is clearly peaked at a nonzero characteristic frequency for any wavelet with at least one vanishing moment. From the scaling property (Eq. 6) it follows, that the frequency at which the peak occurs changes by a factor of two on neighboring resolution grids. This suggest that the coupling between the different resolution levels is weak.

In the preeceding paragraph we presented the mathematical framework only for the one-dimensional case. The generalization to the 3-dim case is straightforward by using tensor products [18]. Also in the rest of the paper only the one-dimensional form of the mathematical formulas will presented for reasons of simplicity. It has to be stressed however that all the numerical results were obtained for the three-dimensional case.

3 The Fourier approach for wavelets

Preconditioning by the diagonal is the simplest preconditioning method. Unfortunately it does not work in most basis sets such as finite elements. Scaling function basis sets are no exception to this rule. It can however be applied if the Laplacian is expressed in a wavelet basis set [19]. Preconditioned conjugate gradient type methods are then a possible method for the solution of Poissons equation expressed in differential form (Eq.1). As discussed above we expect the coupling between different resolution levels to be weak. Within one resolution level the amplitude of the matrix elements should decay rapidly with distance as soon as the wavelet basis functions are not any more overlapping since they represent the interaction of a dipole or higher multipole with other multipoles of the same type. For overlapping basis functions the off-diagonal matrix elements within one block corresponding to one resolution level are presumably not much smaller than the diagonal ones. Nevertheless they are neglected in the current precondition schemes. This neglect is probably the main reason for their relatively slow convergence. The multigrid methods to be discussed later include also in an approximative way through Gauss-Seidel relaxations this off-diagonal coupling within each block.

The matrix elements of the Laplacian in a wavelet basis can be calculated analytically [15]. From the scaling relation (Eq. 6) it follows that they increase by a factor of 4 on each consecutive finer resolution level.

$$\begin{aligned} \int \psi_0^{k+1}(x) \frac{\partial^2}{\partial x^2} \psi_0^{k+1}(x) dx &= 2 \int \psi_0^k(2x) \frac{\partial^2}{\partial x^2} \psi_0^k(2x) dx \\ &= 4 \int \psi_j^k(x) \frac{\partial^2}{\partial x^2} \psi_j^k(x) dx \end{aligned} \tag{12}$$

Hence the preconditioning step using simply the diagonal is given by

$$\Delta V_j^k = const\ 4^{-k} \Delta \rho_j^k \tag{13}$$

In analogy to Eq. 9,10, the $\Delta\rho_j^k$'s are the wavelet coefficients on the k-th resolution level of the residue $\Delta\rho(\mathbf{r}) = \nabla^2\tilde{V}(\mathbf{r}) + 4\pi\rho(\mathbf{r})$ transformed into a wavelet representation. $\tilde{V}(\mathbf{r})$ is the approximate solution at a certain iteration of the solution process. The preconditioned residue ΔV is then used to update the approximate potential $\tilde{V}$. In the case of a preconditioned steepest descent this update would simply read

$$\tilde{V} \leftarrow \tilde{V} + \alpha \Delta V \tag{14}$$

where α is an appropriate step size.

In the 3-dimensional case, the preconditioning is slightly more complicated than in the one dimensional case of Eq. 13. In the 3-dimensional case the diagonal elements of the Laplacian are different for wavelets that are pure products of one-dimensional wavelets or that are products of scaling functions and wavelets. Hence the constant *const* in Eq. 13, that represents the inverse of the diagonal elements of this type of wavelet, is different for the different wavelets that can be formed in the three-dimensional case.

In the following we will present some numerical results for the solution of the 3-dimensional Poisson equation in a wavelet basis using the Fourier approach. All the methods presented in this paper will have the property that the convergence rate is independent of the grid size. We have chosen 64^3 grids for all the numerical examples. The fact that the number of iterations necessary to reach a certain target accuracy is independent of the system size together with the fact that a single iteration involves a cost that is linear with respect to the number of grid points ensures that the Poisson's equation can be solved with overall linear scaling. Whereas we use here only simple equidistant grids, this linear scaling has already been demonstrated with highly adaptive grids in problems that involve many different length scales [6, 7, 8, 9]

Fig. 1 shows numerical results for several wavelet families. The slow convergence of the interpolating wavelets is due to the fact that they have a non-vanishing average and therefore a non-vanishing zero Fourier component [7]. Hence they are all localized in Fourier space at the origin instead of being localized around a non-zero frequency. This deficiency can be eliminated by lifting. The Fourier power spectrum of the lifted wavelets tends to zero at the origin with zero slope for the family with two vanishing moments considered here. The higher 8-th order lifted interpolating wavelet is smoother than its 6-th order counterpart and hence better localized in the high frequency part. This leads to a slightly faster convergence.

Combining the diagonal preconditioning (Eq. 13) with a conjugate gradient minimization instead of a steepest descent minimization gives a significantly faster convergence. The number of iterations can nearly be cut into half for the cases examined above with the steepest descent method.

Up to now we have only considered the case where the elements of the matrix representing the Laplacian were calculated within the same wavelet family that was used to analyze the residue by wavelet transformations to do the preconditioning step. More general schemes can however be implemented. It is not even necessary that the calculation

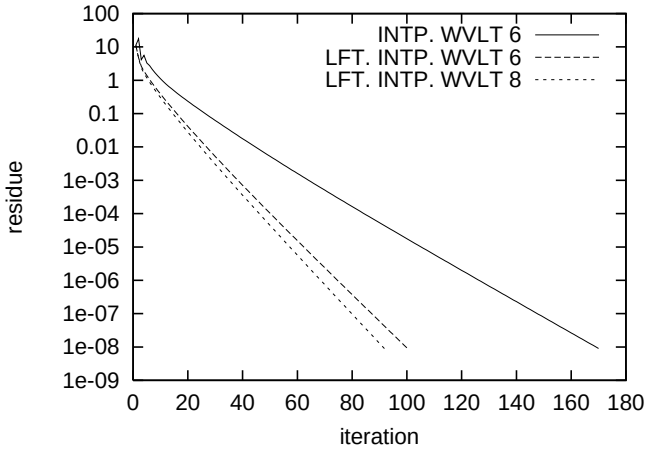

Figure 1: The reduction of the residue during a steepest descent iteration with interpolating and lifted interpolating wavelets.

of the Laplacian matrix elements is done in a wavelet basis. One can instead use simple second order finite differences, which in the one-dimensional case are given by

$$\frac{1}{h^2}(-V_{i-1} + 2V_i - V_{i+1}) \,, \tag{15}$$

or some higher order finite differences for the calculation of the matrix elements. The scaling relation Eq. 12 does not any more hold exactly, but it is fulfilled approximately and the schemes works as well or even better than in the pure wavelet case as is shown in Fig. 2.

4 The FMM approach for wavelets

In the Fourier approach we used an approximate diagonal inverse in the standard representation for preconditioning. We postulated that this is a good approximate inverse because the coupling between different wavelets and in particular between wavelets on different resolution levels should be small. There is another operator representation, the non-standard form[16, 11], where the coupling between the different levels is not contained in the operator representation but hidden in the redundant data representation that is required for its application. This non-standard form might of course also be used to represent an approximate inverse for preconditioning purposes. The non-standard form would have the advantage that we would get an indirect coupling between different levels k even though we do not have to include it in the matrix representation for the approximate inverse. Since the inverse represents the Green's function $\frac{1}{|\mathbf{r}-\mathbf{r}'|}$ the coupling at one resolution level will decay rapidly for the following reasons. On one level k we do not have any coupling in the non-standard representation between scaling functions and scaling functions, but only between scaling functions with wavelets and wavelets with wavelets.

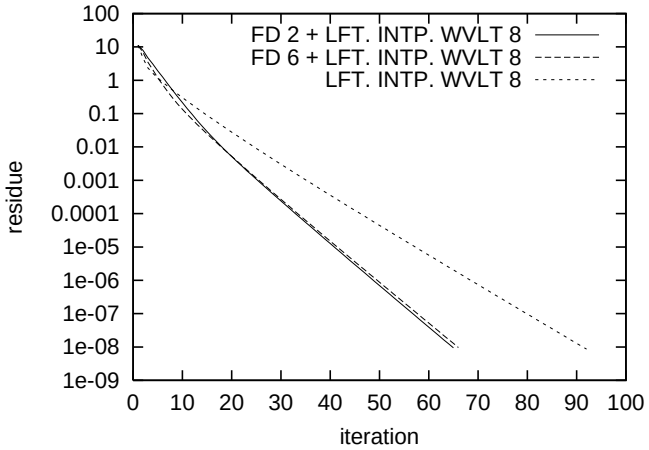

Figure 2: The convergence rate for the case where Poisson's equation is solved with finite differences and 8-th order lifted wavelets are used for the preconditioning step. For comparison the pure wavelet result for the same wavelet family of Fig 1 is reproduced.

The wavelets have in general several vanishing moments, which means that the electrostatic potentials arising from a wavelet charge distribution decays rapidly (e.g. like an octopole). Hence the matrix elements in the non-standard representation decay rapidly away from the diagonal for each of the 3 non-zero blocks.

Let us now point out the similarities between using the non-standard form of the Green's function and the FMM method. Both in the non-standard operator form and in the FMM method successively coarse grained quantities of the charge density are calculated. In the FMM method this is done by calculating multipoles of charge densities formed by particles extending over larger and larger regions, in the non-standard operator form this is done by applying the fast wavelet transform to obtain the redundant representation of the charge density. The representation is redundant since it contains at each resolution level both the wavelet and scaling function coefficients. Both in the non-standard operator form and the FMM method the interactions are then calculated for these redundant quantities. The final step in both methods consists then of calculating the potential in a non-redundant form. In the non-standard operator form this is again done with the help of the fast wavelet transform, in the FMM method again by multipole techniques.

The fast decay of the coupling postulated above sets in only if the basis functions entering into the integral for the matrix element are non-overlapping. In the three-dimensional setting, we are mainly interested in, the number of matrix elements that involve overlapping basis functions is substantial. This comes from the fact that the Green's function $\frac{1}{|\mathbf{r}-\mathbf{r}'|}$ is in contrast to the Laplacian not separable. The number of significant matrix elements is consequently proportional to a three-dimensional volume of a certain radius R_c and not to three times a one-dimensional volume of the same length R_c. For these reasons we have not numerically implemented this approach.

5 The MG approach for wavelets

The aim of this part of the article is twofold. One aspect is how to speed up the convergence of the solution process for Poisson's equation expressed in a wavelet basis set compared to the Fourier approach. The other, and more important, aspect is how to accelerate multigrid schemes by incorporating wavelet concepts. The part therefore begins with a brief review of the multigrid method.

Fig. 3 schematically shows the algorithm of a standard multigrid V cycle [2, 3]. Even though the scheme is valid in any dimension, a two dimensional setting is suggested by the figure, since the data are represented as squares. Since less data are available on the coarse grids, the squares holding the coarse grid data are increasingly smaller. The upper half of the figure shows the first part of the V cycle where one goes from the finest grid to the coarsest grid and the lower half the second part where one goes back to the finest grid.

In the first part of the V cycle the potential on all hierarchic grids is improved by a standard red-black Gauss-Seidel relaxation denoted by GS. The GS relaxation reduces the error of wavelengths λ that are comparable to the grid spacing h very efficiently. In the 3-dimensional case we are considering here, the smoothing factor is .445 (page 74 of ref [2]). Since we use 2 GS relaxations roughly one quarter of the error around the wavelength h survives the relaxations on each level. As a consequence the residue $\Delta\rho$ contains mainly longer wavelengths which then in turn are again efficiently eliminated by the GS relaxations on the coarser grids. Nevertheless, the remaining quarter of the shorter wavelengths surviving the relaxations on the finer grid pollutes the residue on the coarser grid through aliasing effects. Additional pollution is introduced by the restriction operation. Additional means that even if the residue on the finer grid would contain only a wavelength h the restricted quantity would not be identically zero.

In the second part of the V cycle the solutions obtained by relaxation on the coarse grid are prolongated to the fine grids and added to the existing solutions on each level. Aliasing pollution is again present in the prolongation procedure. Due to the accumulated aliasing errors 2 GS relaxations are again done on each level before proceeding to the next finer level.

To a first approximation the different representations of ρ at the top of Fig. 3 represent Fourier filtered version of the real space data set ρ on the finest grid. The large data set contains all the Fourier components, while the smaller data sets contain only lower and lower frequency parts of ρ. Because of the various aliasing errors described above the Fourier decomposition is however not perfect. Obviously it would be desirable to make this Fourier decomposition as perfect as possible. Then the GS relaxations would not have to deal with any Fourier components arising from aliasing errors.

To establish the relation between multigrid and wavelet theory let us first note that the injection scheme for the restriction corresponds to a wavelet analysis step (Eq. 26 of ref. [11]), whereas the standard linear prolongation corresponds to a wavelet synthesis step (formula 27 of ref. [11]) where all the detail or difference coefficients d are set to zero.

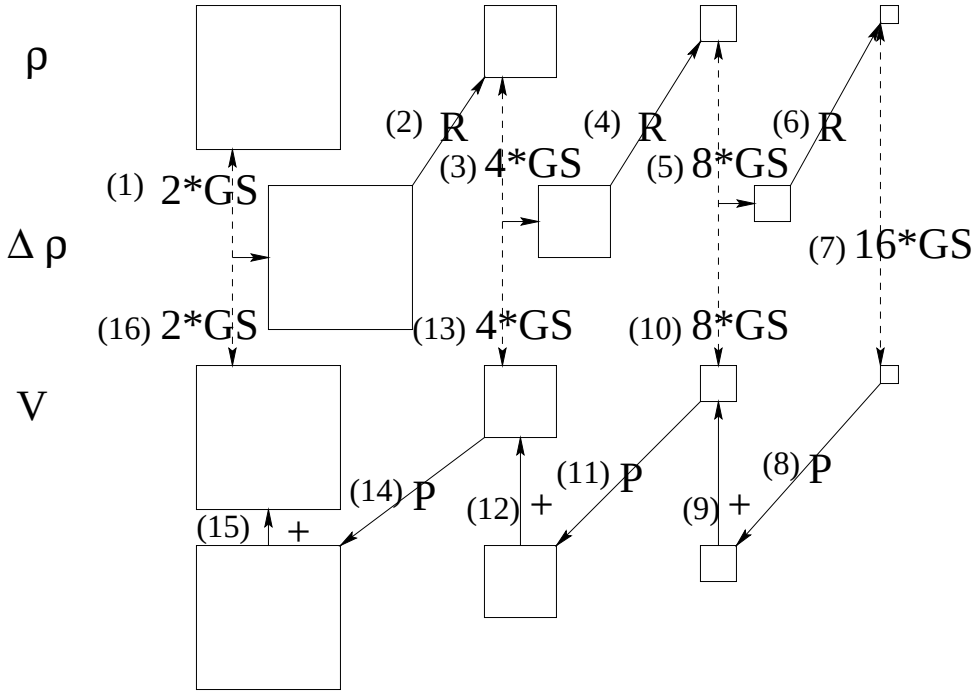

Figure 3: Schematic representation of a multigrid V cycle as described in the text. GS denotes a red-black Gauss-Seidel relaxation, R restriction, P prolongation and + addition of the data sets. The numbering in parentheses gives the ordering of the different steps of the algorithm.

For vanishing d coefficients, the wavelet analysis step is given by

$$s_i^{2h} = \sum_{j=-m}^{m} \tilde{h}_j s_{j+2i}^h \tag{16}$$

and the wavelet synthesis step by

$$\begin{aligned} s_{2i}^h &= \sum_{j=-m/2}^{m/2} h_{2j}\, s_{i-j}^{2h} \\ s_{2i+1}^h &= \sum_{j=-m/2}^{m/2} h_{2j+1}\, s_{i-j}^{2h}\,. \end{aligned} \tag{17}$$

Using the values of the filters $\tilde{h}$ and h for interpolating wavelets we obtain

$$s_i^{2h} = s_{2i}^h \tag{18}$$

and

$$\begin{aligned} s_{2i}^h &= s_i^{2h} \\ s_{2i+1}^h &= \frac{1}{2}\, s_i^{2h} + \frac{1}{2}\, s_{i+1}^{2h}\,. \end{aligned} \tag{19}$$

which is the standard injection and interpolation. As a consequence of the fact that it can be considered as a wavelet forward and backward transformation, the combination of injection and interpolation has the appealing property that applying a restriction onto a prolongation gives the identity.

Usually injection is replaced by the full weightening scheme,

$$s_i^{2h} = \frac{1}{4}\, s_{2i-1}^h + \frac{1}{2}\, s_{2i}^h + \frac{1}{4}\, s_{2i+1}^h \,. \tag{20}$$

This scheme has the advantage that it conserves averages. Applying it to a charge density thus ensures that the total charge is the same on any grid level. Trying to put the full weightening scheme into the wavelet theory framework gives a filter $\tilde{h}$ with nonzero values of $\tilde{h}_{-1} = \frac{1}{4}$, $\tilde{h}_0 = \frac{1}{2}$, $\tilde{h}_1 = \frac{1}{4}$ This filter $\tilde{h}$ does not satisfy the orthogonality relations of wavelet theory (formula 8 of ref. [11]) with the h filter corresponding to linear interpolation. Hence a prolongation followed by a restriction does not give the identity.

A pair of restriction and prolongation operators that conserve averages can however also be derived from wavelet theory. Instead of using interpolating wavelets we have to use lifted interpolating wavelets [13, 12]. In this way we can obtain both properties, average conservation and the identity for a prolongation restriction sequence. Using the filters derived in ref. [11] we obtain

$$s_i^{2h} = -\frac{1}{8}\, s_{2i-2}^h + \frac{1}{4}\, s_{2i-1}^h + \frac{3}{4}\, s_{2i}^h + \frac{1}{4}\, s_{2i+1}^h - \frac{1}{8}\, s_{2i+2}^h \tag{21}$$

$$\begin{aligned} s_{2i}^h &= s_i^{2h} \\ s_{2i+1}^h &= \frac{1}{2}\, s_i^{2h} + \frac{1}{2}\, s_{i+1}^{2h} \,. \end{aligned} \tag{22}$$

The right panel of Fig. 4 shows the convergence rate of a sequence of V cycles for the full weightening/interpolation (Eq. 20,19) scheme and various wavelet based schemes, namely the scheme obtained from second order lifted wavelets (Eq. 21,22), the corresponding scheme, but obtained form 6-th order lifted wavelets (The filters of Eq. 17 and Eq. 16 are $h(-5,...5)$ = 3/256, 0, -25/256, 0, 75/128, 1, 75/128, 0, -25/256 0, 3/256 and $\tilde{h}(-6,...6)$ = -3/1024, 0, 11/512, 0, -125/1024, 1/4, 181/256, 1/4, -125/1024, 0, 11/512, 0, -3/1024) and a scheme obtained from twofold lifted 4-th order interpolating wavelets with 3 vanishing moments ($h(-3,...3)$ = 1/16, 0, 9/16, 1, 9/16, 0, 1/16 and $\tilde{h}(-8,...8)$ = 9/16384, 0, -35/4096, 9/1024, 189/4096, -59/1024, -477/4096, 153/512, 5379/8192, 153/512, -477/4096, -59/1024, 189/4096, 9/1024, -35/4096, 0, 9/16384). Even though these filters are much longer than the ones used in Eq. 20,19,21,22, the CPU time does not increase substantially. This come from the fact that on modern computers the transfer of the data into the cache is the most time consuming part. How many numerical operations are than performed of these data residing in cache has only a minor influence on the timing. The combination injection/interpolation (Eq. 18,19), is not shown since it is much worse, requiring at least the double of the number of iterations for the target accuracy. Since the convergence rate is slightly faster, the new wavelet based schemes for restriction and prolongation are always more efficient than the Full Weightening scheme, both for finite difference discretizations and scaling function basis sets.

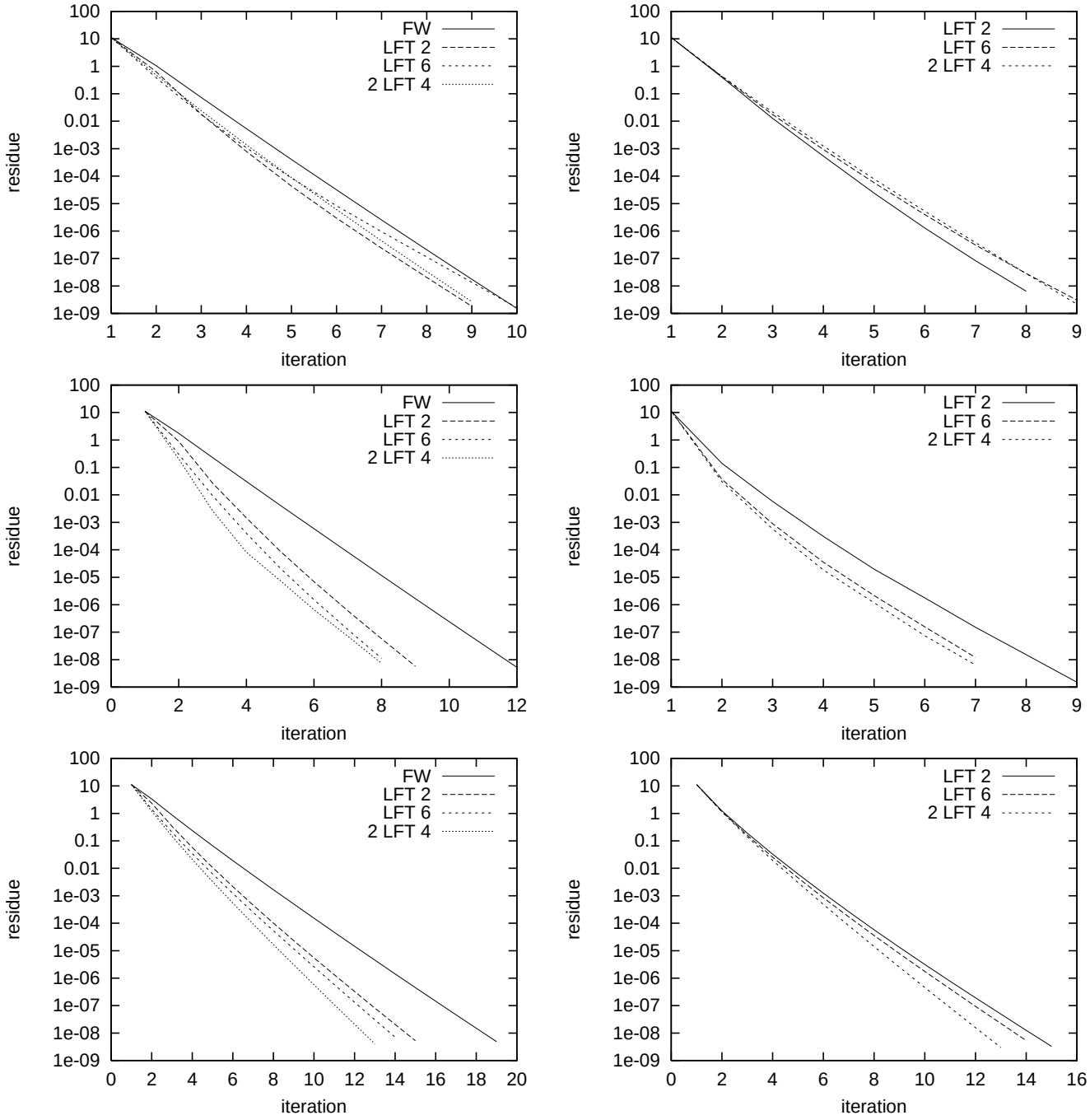

Figure 4: The convergence rate of a sequence of V cycles (left hand side) and halfway V cycles (right hand side). In the upper two plots Poisson's equation was discretized by second order finite differences, In the middle two plots by 6-th order finite differences and in the lower two plots by 6-th order interpolating scaling functions. Shown are results for the Full Weightening scheme (FW) second order lifted wavelets (LFT 2) 6-th order lifted wavelets (LFT 6) and twofold lifted 4-th order wavelets. In the case of ordinary V cycles 2 GS relaxations were done on the finest level both when going up and coming back down, in the case of the halfway V cycle 4 GS relaxation were done on the finest level. The number of GS relaxations was allowed to increase by a factor of 2 on each consecutive coarse grid level.

The main justification for the relaxations in the upper part of the traditional multigrid algorithm shown in Fig. 3 is to eliminate the high frequencies. This can however be done directly by fast wavelet transformations based on wavelets that have good localization properties in frequency space such as lifted interpolating wavelets. As a consequence the traditional multigrid algorithms can be simplified considerably as shown in Fig. 5. Using wavelet based restriction and prolongation operators we can completely eliminate the GS relaxation in the first part of the V cycle where we go from the fine grid to the coarsest grid. We baptize such a simplified V cycle a halfway V cycle. The numerical results, obtained with the halfway V cycle, shown in the right hand plots of Fig. 4, demonstrate that the convergence is slightly faster than for the traditional multigrid algorithm based on the same restriction and prolongation scheme. In addition one step is faster. It is not necessary to calculate the residue after the GS relaxations. Otherwise the number of GS relaxations and restrictions/prolongations is identical in the full and halfway V cycle. On purpose no CPU times are given in this context because optimization of certain routines [10] can entirely change these timings. Because the residue is never calculated in the halfway V cycle, the memory requirements are also reduced by one third.

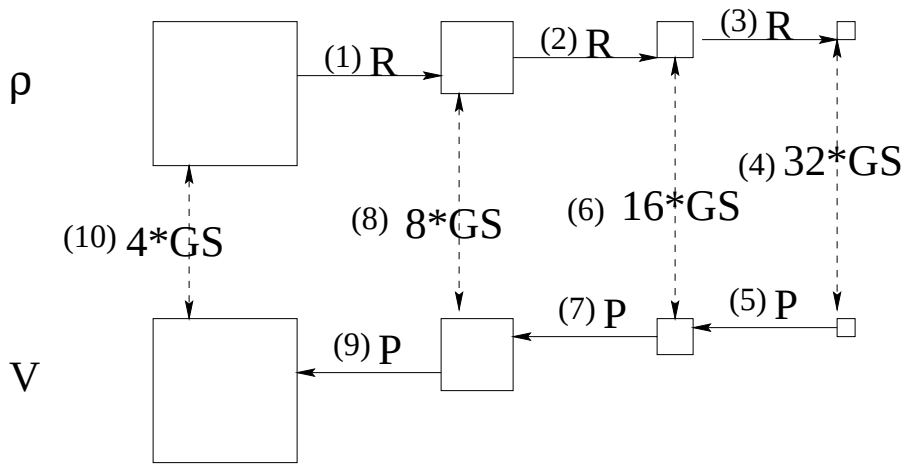

Figure 5: Schematic representation of a halfway V cycle as described in the text. The abbreviations are the same as in Fig. 3.

The number of GS relaxations in the halfway V cycle was chosen to be 4 in order to allow for a entirely unbiased comparison with the traditional V cycle where also 4 GS relaxations were done on the finest grid level. For optimal overall efficiency putting the number of GS relaxation to 3 is usually best, with the values of 2 and 4 leading to a modest increase in the computing time. The convergence rate of halfway V cycles as a function of the number of GS relaxations on the finest grid level is shown in Fig 6. This Figure also shows the influence if the number of GS iterations is held constant on each grid level. The resulting increasing number of iterations is more important than the slightly reduced numerical effort per iteration, leading to roughly a 10 percent increase in the total CPU time.

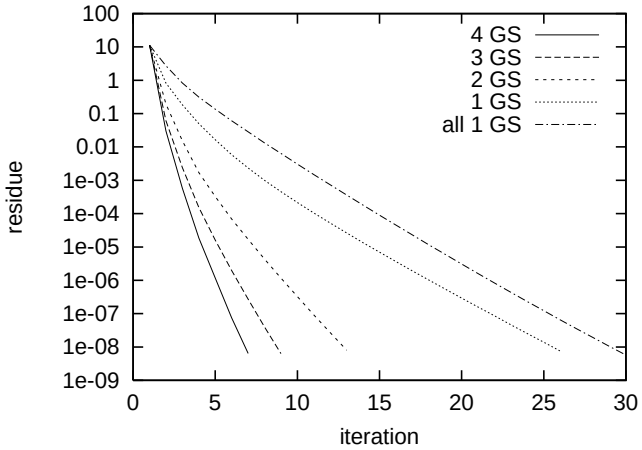

Figure 6: The convergence rate for halfway V cycles with 4, 3, 2 and 1 GS relaxation on the finest grid level where a doubling of the respective number of relaxations is allowed on each additional grid level as well as the convergence rate if 1 GS relaxation is done on all grid levels.

6 Conclusions

Our results demonstrate that halfway V cycles with the restriction and prolongation steps based on wavelet theory are the most efficient approach for the solution of Poisson's equation. It is most efficient both for finite difference discretizations and for the case where scaling functions or wavelets are used as basis functions. We expect that the approach should also be the most efficient one in connection with finite elements. It is essential that the wavelet family used for the derivation of the restriction and prolongation schemes has at least one vanishing moment and conserves thus average quantities on the various grid levels. Wavelet families with more vanishing moments lead only to a modest increase of the convergence rate compared to the case of one vanishing moment. Orthogonality is not a beneficial feature in this context [17] and therefore interpolating wavelets were used instead of Daubechies wavelets. In addition to its increased efficiency in terms of the CPU time, the proposed halfway V cycle algorithm is also considerably simpler than the standard V cycle. This makes not only programming easier, but also reduces the memory requirements.

7 Acknowledgments

I thank Achi Brandt for sharing with me his great insight on multigrid methods.

References

[1] L. Greengard and V. Rokhlin, J. Comp. Phys., **73**, 325 (1987) ; L. Greengard, Science, **265**, 909 (1994)

[2] U. Trottenberg, C. Oosterlee, A. Schüller, *"Multigrid"*, Academic Press, San Diego, CA, 2001

[3] W. Hackbusch and U. Trottenberg, *"A Multigrid Methods"*, Springer, Berlin, 1982 ; W. L. Briggs, *"A Multigrid Tutorial"*, SIAM, Philadelphia, PA, 1987

[4] C. White, B. Johnson, P. Gill and M. Head-Gordon, Chem. Phys. Lett. **230**, 8 (1994) ; M. Strain, G. E. Scuseria and M. Frisch, Science **271**, 51 (1996) ; Perez-Jorda, J., and W. Yang, J. Chem. Phys. **107**, 1218 (1997) K. N. Kudin and G. E. Scuseria, J. Chem. Phys. **111**, 2351 (1999) ; K. N. Kudin and G. E. Scuseria, Phys. Rev. B **61**, 16440 (2000) ;

[5] A. Brandt, Mathematics of Computation **31**, 333 (1977)

[6] S. Goedecker, O. Ivanov, Sol. State Comm., **105** 665 (1998)

[7] S. Goedecker, O. Ivanov, Comp. in Phys, **12**, 548 (Nov/Dec 1998)

[8] R. A. Lippert, T. Arias and A. Edelman, J. Comp. Physics, **140**, 278 (1998)

[9] T. A. Arias, Rev. Mod. Phys. 71, **26**7 (1999)

[10] S. Goedecker, A. Hoisie, *Performance Optimization of numerically intensive codes*, SIAM publishing company, Philadelphia, USA 2001 (ISBN 0-89871-484-2)

[11] S. Goedecker: "Wavelets and their application for the solution of partial differential equations", Presses Polytechniques Universitaires et Romandes, Lausanne, Switzerland 1998, (ISBN 2-88074-398-2)

[12] R. Schneider: *"Multiskalen- und Wavelet-MatrixKompression"*, Teubner publishing, Stuttgart 1998

[13] W. Sweldens, *Appl. Comput. Harmon. Anal.* **3**, 186 (1996).

[14] G. Deslauriers and S. Dubuc, *Constr. Approx.* **5**, 49 (1989).

[15] G. Beylkin, *SIAM J. on Numerical Analysis* **6**, 1716 (1992).

[16] G. Beylkin, R. Coifman and V. Rokhlin, *Comm. Pure and Appl. Math.*

[17] A. Brandt, Multiscale Scientific Computation: Review 2000, http://www.wisdom.weizmann.ac.il/ achi/

[18] I. Daubechies, *"Ten Lectures on Wavelets"*, SIAM, Philadelphia (1992)

[19] Jaffard (1992)